

Transport properties of $\text{Bi}_2\text{Sr}_2\text{Ca}_{n-1}\text{Cu}_n\text{O}_{2n+4}$ thin films

M. Viret and J. M. D. Coey

Department of Pure and Applied Physics, Trinity College, Dublin 2, Ireland

(Received 25 June 1993; revised manuscript received 10 September 1993)

The Hall effect and resistivity have been measured in $\text{Bi}_2\text{Sr}_2\text{Ca}_{n-1}\text{Cu}_n\text{O}_{2n+4}$ ($n=2$ and 3) thin films as a function of magnetic field and temperature. In the normal state, the ratio of the normal resistivity to the Hall resistivity (the cotangent of the Hall angle) is found to vary as T^2 . Three models are able to account qualitatively for such behavior: a bipolaron model, BCS with a Van Hove singularity, and resonating valence bond. Analyses of the resistivity and the Hall effect in the superconducting fluctuations region above T_c clearly demonstrate the two-dimensional character of the 2:2:1:2 compound. The sign reversal of the Hall constant in the vortex state is related to vortex motion. An explanation is presented based on the motion of an antivortex, or a defect of the local vortex lattice, in moving vortex bundles. The calculated activation energy of approximately 730 K agrees well with the measured value of 750 K, and the model gives the correct sign for the Nernst effect.

I. INTRODUCTION

The transport behavior of copper oxide high-temperature superconductors (HTSC's) is rather unusual.¹⁻⁹ In particular, Hall-effect measurements provide a challenging test to theories. The variation of the Hall constant R_H with temperature is unexpected both in the normal state (above T_c) and in the vortex state (below T_c). Various explanations have been proposed for the Hall effect and resistivity, but there is still no universally recognized model able to account for the variations of R_H with temperature and magnetic field. Here we present data on the Hall effect and resistivity of Bi-Sr-Ca-Cu-O films in the normal state, in the region of superconducting fluctuations just above T_c , and in the vortex state below T_c where the Hall voltage changes sign. Results are discussed in relation to the two-dimensional structure of the compounds and an idea is proposed to account for the sign reversal of R_H below T_c .

II. EXPERIMENT

Thin films of the $\text{Bi}_2\text{Sr}_2\text{Ca}_{n-1}\text{Cu}_n\text{O}_{2n+4}$, $n=2$ and 3 , compounds were synthesized by pulsed laser deposition, using two crystallization methods: *in situ* and post-deposition annealing (*ex situ*). The results obtained by these two methods are reported elsewhere.⁹ The films used had the following characteristics: The *ex situ* 2:2:1:2 films are single phase, 3000 Å thick, and display a sharp drop in resistivity at 83 K followed by a long low-resistivity tail at lower temperature leading to zero resistivity (defined as $\rho_{\text{zero}} = 10^{-5}\rho_{\text{RT}}$) at 68–73 K. The *in situ* crystallized 2:2:1:2 films have better surface quality and good crystallographic properties. Their typical thicknesses are around 700 Å, but their resistive transitions are broader than those of the post-annealed films and of a different nature. The transition itself is quite broad and the resistive tail at lower temperatures very

short. We have suggested that this could be due to inhomogeneities in oxidization induced by the method of synthesis.⁹ The best temperature of zero resistivity obtained for a 2:2:1:2 film is 73 K. The 2:2:2:3 films, prepared by post-annealing treatments, contain a significant amount of the 2:2:1:2 phase. Their resistivities display sharp drops at 110 K to small but nonzero values, followed by a second transition typical of the presence of the 2:2:1:2 phase.

Resistivities and Hall-effect measurements were carried out with dc current densities of the order of 100 A/cm². The films for Hall-effect measurements were etched into a bar shape with five contacts (Fig. 1). For each step in temperature, the resistive bridge is first adjusted in zero field to give strictly zero Hall voltage. Then a 1.2-T field is turned on, and the difference taken between measurements with both senses of the field eliminate the longitudinal resistive component.

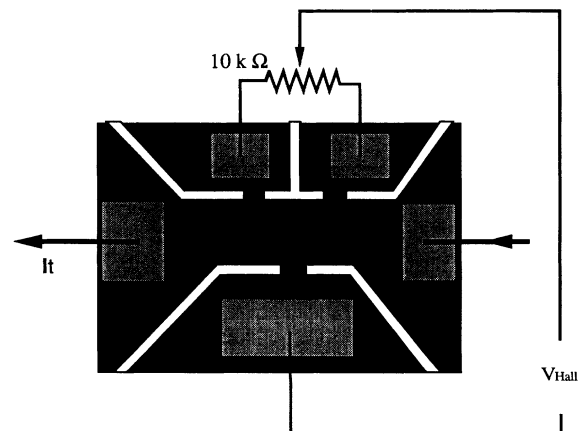


FIG. 1. Five-contact bar shape etched on the films for Hall-effect measurements.

III. RESULTS AND DISCUSSION

The three types of thin films (the *ex situ* 2:2:1:2 and 2:2:2:3 and the *in situ* 2:2:1:2) gave qualitatively the same results for their transport properties. Their resistivities are approximately linear in the normal state. At T_c the resistivities fall abruptly to nonzero values and are followed by tails at lower temperatures. The Hall constants are positive and display a $1/T$ dependence in the normal state. At T_c they drop sharply to large negative values before increasing progressively with further decrease of the temperature to reach values below detection threshold at around $T_c/2$. A typical Hall-effect curve, obtained on *ex situ* 2:2:1:2 films, is presented in Fig. 2. Since our contacts on *in situ* films were of poorer quality, the curves obtained are more noisy, but they are nevertheless qualitatively the same. A precise quantitative analysis could only be carried out on *ex situ* films.

A. Normal-state properties

Above T_c the resistivity and Hall constant are independent of magnetic field and current. Figure 3 displays the temperature dependence of the cotangent of the Hall angle (i.e., ρ_{XX}/ρ_{XY}) for the three types of films. For all samples, $\cot(\theta_H)$ is proportional to the square of the temperature. Moreover, it is striking that the slopes of the straight-line fits to the different samples are very similar (the average T^2 coefficient is found to be 0.075 K^{-2}), although the slopes for the resistivity and Hall number can be quite different. This suggests that the Hall angle is a more meaningful quantity than the Hall constant. This result is consistent with data reported for Y-Ba-Cu-O (Ref. 7) and Bi-Sr-Ca-CuO (Ref. 8) monocrystals. Studies carried out with doping species (see, for example, Ref. 8) demonstrate that this property is common to all superconducting samples. Such behavior can be explained in terms of theories which predict a T dependence for the resistivity and a $1/T$ dependence for the Hall constant, namely, bipolaron models,¹⁰ BCS models with a Van Hove singularity,¹¹ and resonating-valence-bond (RVB) models.¹² In particular, results on Y-Ba-Cu-O (Ref. 7) have been discussed in the framework of the RVB theory. Also, the results on Bi-Sr-Ca-Cu-O (Ref. 8) were explained by a single-band Fermi-liquid model with a nest-

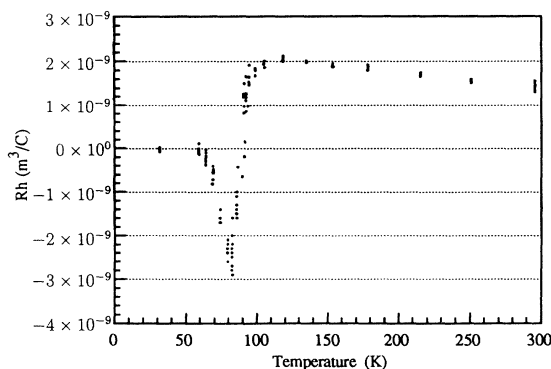


FIG. 2. Variation of the Hall constant R_H with temperature for an *ex situ* 2:2:1:2 film.

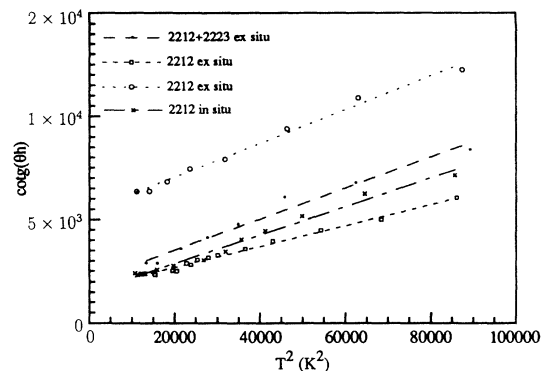


FIG. 3. T^2 dependence of the cotangent of Hall angles measured in films synthesized *in situ* and *ex situ*.

ed Fermi surface, otherwise unable to account for high- T_c superconductivity. Since the three theories mentioned above make the same qualitative predictions, further studies on the quantitative implications of the models for transport properties are necessary to clarify the behavior of HTSC's in the normal state and the origin of superconductivity in these compounds. It is worth pointing out that recent photoemission measurements¹³ have provided evidence for the existence of a singularity in the electronic density of states of HTSC's near the Fermi level. Transport measurements in the normal state are therefore consistent with the explanation of high- T_c superconductivity based on the BCS theory in materials presenting a Van Hove singularity in their density of states, as first proposed by Labbé and Bok.¹⁴

B. Superconducting fluctuations

1. Resistivity

Superconducting fluctuations in the resistivity of layered compounds give rise to an excess conductivity above T_c which is apparent in the deviation from linearity of the $\rho(T)$ curve. Figure 4 presents the variation of the inverse of the excess conductivity as a function of temperature.

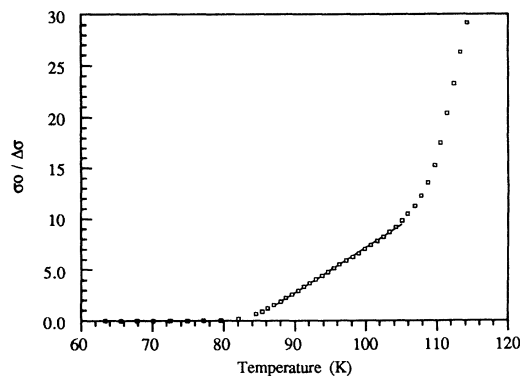


FIG. 4. Determination of T_c from 2D fluctuation studies of the resistivity of *ex situ* 2:2:1:2 films (σ_0 is the conductivity at room temperature).

The superconducting fluctuations were analyzed in the model developed by Lawrence and Doniach.¹⁵ This model is based on the Aslamazov-Larkin fluctuations taking place in superconducting layers coupled by Josephson tunneling. The fluctuation of the order parameter corresponds to the appearance of superconducting pairs of limited lifetime which induce an excess of conductivity. This model is particularly well suited to Bi-Sr-Ca-Cu-O superconductors,^{16,17} which are clearly two-dimensional materials. The resulting expression for the excess conductivity is

$$\Delta\sigma = (e^2/16hd)\varepsilon^{-1/2}\{\varepsilon + 4[\xi_c(0)/d]^2\}^{-1/2}, \quad (1)$$

where ε is the reduced temperature, $\varepsilon = [(T/T_c) - 1]$, d the distance between the superconducting layers, and $\xi_c(0)$ the coherence length along the direction normal to the planes in zero field.

For two-dimensional (2D) systems where the superconducting layer spacing is much larger than the coherence length, this expression becomes

$$\Delta\sigma_{2D} = (e^2/16hd)\varepsilon^{-1}. \quad (2)$$

The critical temperature was therefore found by linear extrapolation of the excess conductivity plot. For the film of Fig. 4, T_c is found to be 83.5 K.

To verify the dimensionality of the system, the excess conductivity is then plotted versus the reduced temperature on a log-log scale in Fig. 5. The slope measured on this curve is 1.01, demonstrating a two-dimensional character. The d space found from Eq. (2) is 8.5 Å. This value may not be precisely representative of the real spacing between the superconducting sheets because the granular character of the films has not been taken into account, but it is certainly of the right order of magnitude. The analysis of superconducting fluctuations using a granular model would lead to lower values for the measured d spacing without altering the exponent in Eq. (2).^{16,18} In any case, the measurement clearly demonstrates the 2D electronic character of 2:2:1:2 compounds. Similar results have been published for Bi-Sr-Ca-Cu-O bulk samples¹⁹ and thin films synthesized by liquid-phase epitaxy²⁰ and laser ablation.^{16,17} The dimensionality of the 2:2:1:2 and 2:2:2:3 systems is systematically found to be 2,

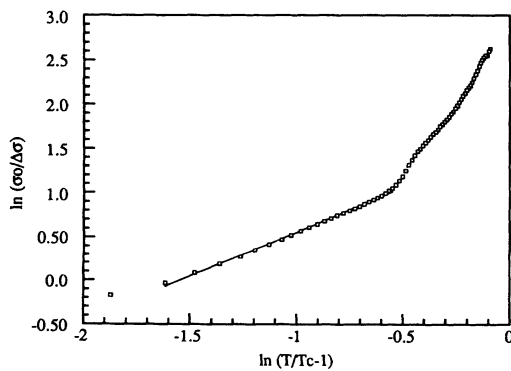


FIG. 5. Evidence of the 2D character of superconducting fluctuations of the resistivity of *ex situ* 2:2:1:2 films on a $\log(\sigma_0/\Delta\sigma)$ vs $\log_{10}(t-1)$ curve.

and the coherence lengths inferred for the 2:2:1:2 compound range from 3.2 Å (in Ref. 16, using a granular model) to about 19 Å (in Ref. 17, without taking impurities into account). It is not entirely clear in the 2:2:1:2 structure whether the spacing of the superconducting planes should be taken as 3.5 Å (the distance between two adjacent CuO_2 planes) or 15.4 Å (half the crystallographic cell height).

2. Hall effect

The superconducting fluctuations in our Hall-effect measurements were analyzed using the model developed by Fukuyama, Ebisawa, and Tsuzuki for conventional superconductors,²¹ again based on the Aslamazov-Larkin fluctuations. Their expression for the excess conductivity depends on the dimensionality of the system, n , as

$$\Delta\sigma_{XY} \propto [(T/T_c) - 1]^{-(3-n/2)}. \quad (3)$$

As in the analysis of the resistivity curve, the normal-state behavior has to be subtracted in order to obtain the excess conductivity. Here the shape of the Hall conductivity in the normal state is taken to be proportional to $1/T$. The excess Hall conductivity thus obtained is plotted in Fig. 6 versus the reduced temperature on a logarithmic scale. The slope of the linear fit is -2.06 , leading to a value for the dimensionality of the system of 1.9. We are not aware of any other result on the excess Hall conductivity on Bi-Sr-Ca-Cu-O thin films. The two-dimensional character demonstrated by the resistive fluctuations is thus independently confirmed by Hall-effect measurements.

C. Vortex-state properties

1. Resistivity

The resistive transition is broadened in an applied magnetic field. Resistivities in the vortex state can be expressed as a thermally activated quantity of the form¹

$$\rho = \rho_0 \exp(-U/k_B T),$$

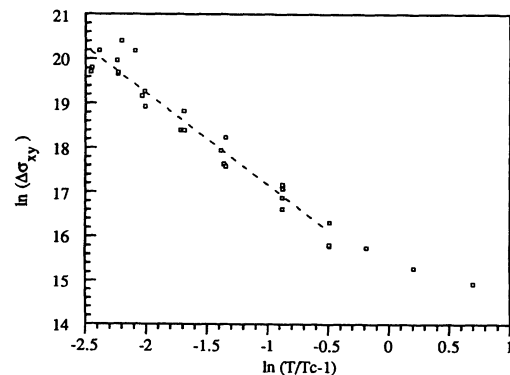


FIG. 6. Evidence of the 2D character of superconducting fluctuations of the Hall effect of *ex situ* 2:2:1:2 films. The dimensionality obtained with the Fukuyama-Ebisawa-Tsuzuki theory is 1.9.

where U is the activation energy and ρ_0 the resistivity just above T_c .

The activation energies of *in situ* and *ex situ* films are found to behave differently, as shown on Fig. 7. The *ex situ* films present a cusp in their $U(T)$ curves which has previously been observed in monocrystals.¹ Such behavior is not observed for *in situ* films whose activation energies can be well fitted by a monotonic T dependence. Also, activation energies are larger for *in situ* films than for *ex situ* ones. The broadening of resistivities with an applied field of 1.2 T is therefore much smaller for *in situ* films. A typical numerical expression obtained for the resistivity of *in situ* films is

$$\rho = 480 \exp[-600(-\varepsilon)^{2/3}/T] \quad (\mu\Omega \text{ cm}),$$

with $-\varepsilon = 1 - T/90$.

The corresponding expression obtained for *ex situ* films in the "visible region" of the resistivity, i.e., above 45 K, is

$$\rho = 530 \exp[-190(-\varepsilon)^{1/2}/T] \quad (\mu\Omega \text{ cm}),$$

with $-\varepsilon = 1 - T/82$.

In the temperature range $50 < T < 80$ K, the resistivity does not depend on the current. Magnetoresistance measurements carried out on *ex situ* films showed that the resistivity is dependent on applied field in the vortex state. A typical $\rho(B)$ curve is presented in Fig. 8. It consists of a strong increase at low fields followed by saturation at higher fields. We studied the low-field behavior in more detail (below the saturation) and found a $B^{1/4}$ variation over a wide range of temperatures. The final empirical expression for the resistivity above 45 K for low magnetic fields can be written as

$$\rho = 530 \exp[-200(-\varepsilon)^{1/2}/(B^{1/4}T)] \quad (\mu\Omega \text{ cm}),$$

with $-\varepsilon = 1 - T/82$.

2. Hall effect

The Hall effect changes its sign in the vortex state from positive to negative. The Hall voltage is also field dependent, and its variation is shown in Fig. 9 at a temperature of 70 K. The Hall voltage is below our measurement

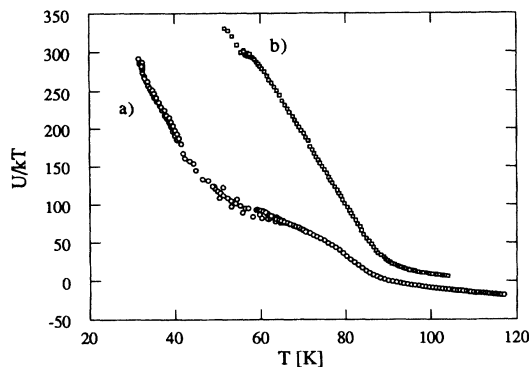


FIG. 7. Variation of activation energies with temperature for (a) an *ex situ* 2:2:1:2 film and (b) an *in situ* 2:2:1:2 film.

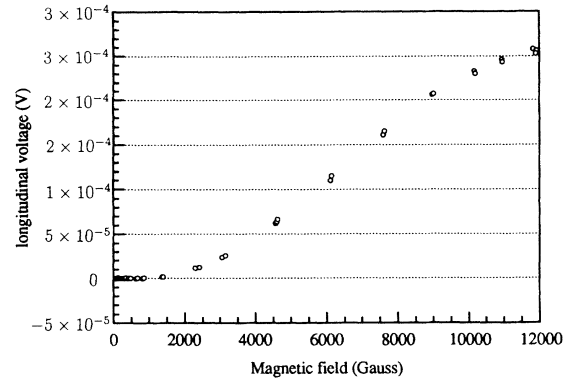


FIG. 8. Variation of the resistivity with magnetic field for an *ex situ* 2:2:1:2 film.

threshold until the field reaches a certain value, where V_H starts decreasing in negative values.

We have plotted in Fig. 10 on a log-log scale, the variation of $-\rho_{XY}$ as function of the corresponding resistivity ρ_{XX} as inferred from the $R(T)$ curves. As suggested in Ref. 22, we tried to find out if the Hall resistivity could be expressed as a power of the longitudinal resistivity. Indeed, in our two best *ex situ* films, the Hall effect is well described by a power dependence of the resistivity with an exponent of 2.8. Luo, Orlando, and Graybeal⁴ found 1.7 for their YBCO monocrystal, in good agreement with the predictions of the vortex-glass theory. However, the 2:2:1:2 compound is not expected to undergo a vortex-glass transition, and the exponent should therefore be 1, as already measured on monocrystals.²³ We are not aware of any values measured on thin films. However, it is likely that the 2.8 found here has no intrinsic physical meaning, but rather characterizes the granularity of *ex situ* films.

It is also possible to express the Hall constant as a thermally activated variable. Figure 11 shows the Arrhenius plot of $-\rho_{XY}$ in the vortex state. The activation energy is found to be $U_H/k_B = 750$ K.

The sign reversal of the Hall effect in the mixed state of HTSC's is related to vortex motion.³ Some explanations

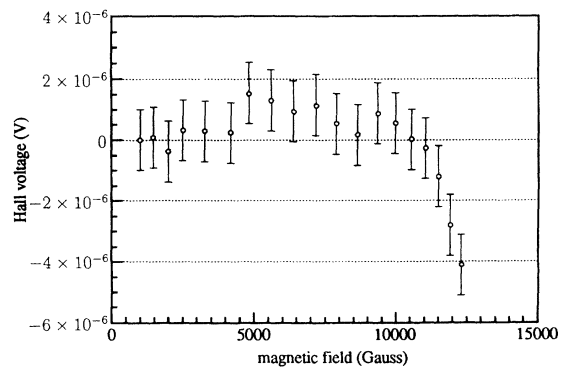


FIG. 9. Variation of Hall voltage as a function of magnetic field for an *ex situ* 2:2:1:2 film.

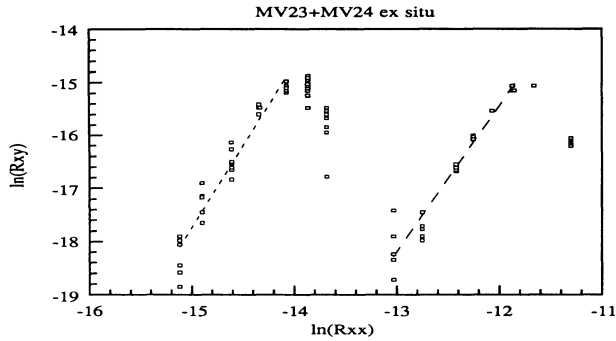


FIG. 10. Hall resistivity as function of longitudinal resistivity for the two best *ex situ* 2:2:1:2 films on a log-log scale. The slope is found to be 2.8.

have been proposed which are based on a backflow component in the motion³ or on thermomagnetic effects associated with the mainly transversal vortex motion.²⁴ It is important to note that these models are all based on single, isolated vortex motion. Here we would like to suggest a different explanation which is based on the influence of the vortex interactions in these temperature and field ranges on the motion of single vortices. Recently, a model taking into account vortex interactions was established by Jensen *et al.*²⁵ In what follows, we will compare our predictions with theirs. We first assume that the mechanism for the sign reversal of the Hall effect is the same for *all* HTSC's, and we use the results of Chien *et al.*⁵ who studied the mixed-state properties of the magnetoresistance and Hall effect of Y-Ba-Cu-O monocrystals. They found evidence for two regimes of vortex motion: At low fields, the vortex motion is correlated over very large volumes. At a field corresponding to the minimum in the Hall effect, this correlated vortex phase makes a transition to a second state in which the motion is diffusive (the vortices interact weakly in a disordered potential with average barrier heights smaller than kT) and the Hall effect increases to positive values. This picture suggests that the negative part of the Hall effect is linked to *collective vortex motion*. Recent results on the magnetoresistance of 2:2:1:2 single crystal in the

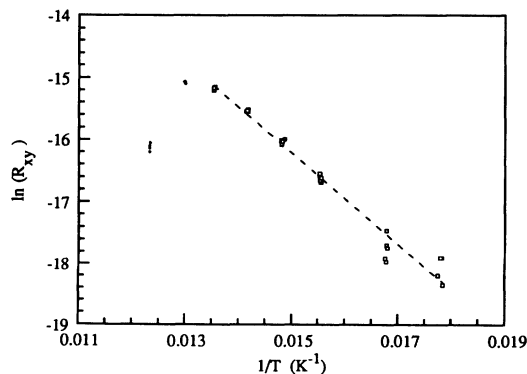


FIG. 11. Arrhenius plot of the Hall constant with temperature in the vortex state of an *ex situ* 2:2:1:2 film. The activation energy obtained is 750 K.

vortex state were used by Artemenko, Gorlova, and Latshev²⁶ to define a region in the (H, T) plane where the Abrikosov vortex lines along c are broken by thermal fluctuations and transport current leading to two-dimensional vortices moving along the layers. The Ohmic behavior of our current-voltage curves in the region of negative Hall effect further indicates that, in this range of temperature, field, and current, 2D "pancake" vortices can be formed.

Based on these results on the vortex-state properties of HTSC's, we consider a model where *bundles* of 2D vortices move under the effect of an applied current, the local vortex lattice remaining intact within the bundles. The Nozières-Vinen²⁸ and Bardeen-Stephen²⁹ models of *single* vortex motion predict a positive Hall angle which cannot explain the observed sign reversal. We therefore suggest that the negative component can be understood by considering the motion of *vacancies or antivortices* on the 2D lattice within the bundles. We postulate here the existence of an equilibrium concentration of vacancies by analogy with other defects in a solid or thermally generated antivortices (vortex-antivortex pairs in fact, but it was shown that the antivortex is the only one contributing to the dissipation process²⁵). We show that their motion can lead to a negative Hall effect and an activation energy, in good agreement with the measured values.

It is convenient to represent a vacancy as the superposition of a vortex in a bundle of defect-free lattice with an antivortex of opposite flux direction. By analogy with electrons and holes in semiconductors, a vortex hopping into a vacancy is equivalent to the opposite motion of an antivortex on a defect-free lattice. The process of *free antivortex motion* illustrated in Fig. 12 generates a negative Hall voltage.

Such a motion can be described as a thermally activated process, where the activation energy is given by the barrier the antivortex must overcome to jump from one site to the neighboring one. We use the following expression²⁷ for the interaction energy between a 2D vortex-antivortex pair:

$$U(r_{ij}) = \phi_0^2 d / (8\pi^2 \lambda_{ab}^2) \ln(r_{ij} / \xi),$$

where d is the coherence length of a vortex along the field, λ_{ab} is the penetration depth in the a, b plane, ξ is the coherence length in the a, b plane, and r_{ij} is the dis-

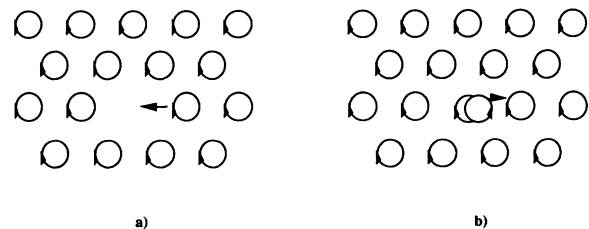


FIG. 12. (a) Bundle of vortices containing a defect (vacancy), compared to (b) a defect-free lattice bundle with an antivortex. Hopping of a vortex in (a) to the left is equivalent to motion of the antivortex in (b) to the right.

tance between vortex and antivortex.

To calculate the barrier height, we consider the action of all the vortices in the ellipse of Fig. 13(b) on the antivortex. The activation energy is then given by the

$$U_1 = \phi_0^2 d / (16\pi^2 \lambda_{ab}^2) [0 + 6 \ln(a_0^2 / \xi^2) + 4 \ln(3a_0^2 / \xi^2) + 3 \ln(4a_0^2 / \xi^2)] ,$$

where a_0 is the vortex lattice spacing, $a_0^2 = 2\phi_0 / \sqrt{3}B$, whereas the corresponding energy in Fig. 13(b) is

$$U_2 = \phi_0^2 d / (16\pi^2 \lambda_{ab}^2) [2 \ln(a_0^2 / 4\xi^2) + 2 \ln(3a_0^2 / 4\xi^2) + 4 \ln(7a_0^2 / 4\xi^2) + 2 \ln(9a_0^2 / 4\xi^2) + 4 \ln(13a_0^2 / 4\xi^2)] .$$

The energy barrier is obtained as the difference between these two energies:

$$U = U_2 - U_1 = \phi_0^2 d / (16\pi^2 \lambda_{ab}^2) \{ \ln(a_0^2 / \xi^2) - [34 \ln(2) - 2 \ln(3) - 4 \ln(7) - 4 \ln(13)] \} \\ = \phi_0^2 d / (16\pi^2 \lambda_{ab}^2) \{ \ln[(2\phi_0 / \sqrt{3}B) / \xi^2] - 3.35 \} .$$

With typical numerical values of $\lambda = 1300 \text{ \AA}$, $\xi = 10 \text{ \AA}$, $d = 15 \text{ \AA}$, and $B = 1.2 \text{ T}$, we find $U/k_B = 730 \text{ K}$, which is in good agreement with the value of 750 K measured from the Hall-effect curve (Fig. 11). In this calculation, we have neglected the out-of-plane interactions and we took the height d of these 2D vortices as half the 2:2:1:2 unit cell.^{26,27}

The presence of vacancies, or antivortices, in the Abrikosov lattice could come from unbinding of vortex-antivortex pairs²⁵ by the applied current or magnetic field below the Kosterlitz-Thouless (KT) transition temperature (where all bound pairs spontaneously dissociate). Indeed, it should be pointed out that the negative Hall effect was also observed in thin films of classical superconductors,³ where the KT mechanism of vortex-

difference in energy between the situations in Figs. 13(a) and 13(b) where the antivortex is halfway between the two vortex sites. The interaction energy in Fig. 13(a) is given by

antivortex unbinding is present. In addition, it is interesting to note that other defects in the Abrikosov lattice such as dislocations (which have been suggested to be at the origin of the lattice melting³⁰) could also give rise to a negative component of the Hall effect. But any negative contribution must overcome the positive signal induced by the motion of the flux bundles. Qualitatively, this could only be achieved if the Hall angle for antivortex motion were quite large compared to that of vortex-bundle motion. This assumption is plausible since the mobility and viscosity coefficient of the antivortex could be very different from those of a vortex bundle (which depends on its friction with the crystal and impurities). Some further theoretical work is needed to quantify the different contributions.

We now compare our model of mobile defects in moving vortex bundles with the work of Jensen *et al.*²⁵ who presented a model of antivortex motion to explain the sign reversal of the Hall effect in the mixed state. They consider the motion of thermally dissociated vortex-antivortex pairs on a pinned lattice of magnetically induced vortices and demonstrate that the antivortices are mainly responsible for the dissipation in the mixed state. However, their model should lead to a sign for the Nernst effect in the mixed state opposite to that observed.^{31,32} The Nernst effect describes the transverse electric field generated by a temperature gradient. It gives information on the entities carrying entropy which move down the temperature gradient. The sign of the Nernst voltage in HTSC's is evidence of vortex motion.³¹ We can resolve this problem by considering that the antivortices or defects move on a background of moving vortex bundles. In this case, the Hall and Nernst effects are a combination of two opposite contributions from vortex and antivortex motion. In fact, the Nernst effect, like the resistivity, is sensitive to transverse motion, perpendicular to the current lines, whereas the Hall effect is due to the longitudinal component of the motion. We argue that the entities responsible for the former effects are bundles of vortices, but that antivortices represent the main component of the latter. In fact, Jensen *et al.* themselves demonstrate that antivortices are highly mobile on the vortex lattice. The viscosity of the vortex bundles, when the first vortices (antivortices) are depinned in this field

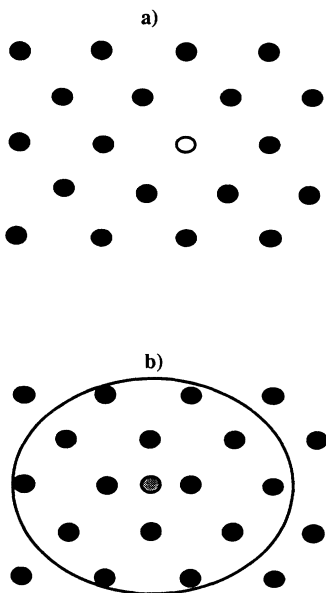


FIG. 13. Antivortex motion in a vortex lattice bundle: The energy barrier is given by the difference in energy between (b) and (a) situations. The calculation is made by considering the interaction between the antivortex and vortices contained in the ellipse of (b).

and temperature regimes, can be very large. In the case of a “two-band” contribution for transport, it is well known that the higher the mobility of the carrier in one band, the larger its Hall angle.

The reproducible and field-independent negative sign for the Nernst effect^{31,32} at low temperatures (see in particular Figs. 1 and 2 in Ref. 31) is evidence for the validity of our model. This small negative region before the positive peak corresponds to the state described by Jensen *et al.* where the vortex lattice is pinned and the entities moving are the thermally generated vortex-antivortex pairs. In this case, antivortices are indeed mainly responsible for the dissipation. Then, at slightly higher temperatures, the vortex lattice begins to be depinned, and bundles start to move with a very low mobility, hence generating the positive Nernst voltage.

Another problem in the predictions of Jensen *et al.* is their calculation of the activation energy associated with the antivortex motion process. They argue that, in order for the pair to dissipate energy, the antivortex has to be annihilated by a vortex other than its pair companion and therefore that only those pairs created with a separation of the order of a_0 can participate in the net transport process. They deduce from this that the energy barrier should be of the order of the potential energy of a pair separated by a_0 . We argue that this activation energy is incorrect because it takes no account of the influence of the other vortices of the lattice. We think that the correct activation energy is close to the one we obtained above for free antivortex motion. The energy necessary to separate the pair in the vortex lattice background should be quite close to the one corresponding to Fig. 13 since Jensen *et al.* demonstrated that the process associated with the lattice relaxation around the vortex (which does not dissipate energy) is on a much faster time scale than the antivortex motion. Therefore the shape of the local lattice must change during the separation process to reach the configuration of Fig. 13(b) where the pair can be considered broken. The total energy necessary to generate this independent antivortex is then approximately the sum of our separation energy with the condensation energy of the two normal cores of the pair. This latter contribution only amounts to less than 10 K, which makes the total activation energy close to the 750 °C measured here. Moreover, we also expect it to be the same for the resistivity since defect generation will help depinning trapped vortices and will therefore induce motion in the vortex lattice.²⁵

In order to test our model, it would be necessary to measure magnetoresistance and Hall and Nernst effects as functions of pinning in these materials. In particular, the pinning strength should control the Hall and Nernst behaviors since it directly affects the relative importance of motion of flux bundles and individual vortices. For example, since it is known that Ni doping or ion bombardment increase pinning, it would be interesting to compare

the transport properties in the mixed state of samples with different doping composition or radiation doses.

IV. CONCLUSIONS

Transport properties of thin films of the Bi-Sr-Ca-Cu-O high-temperature superconductor have been measured as function of temperature and magnetic field. Coherent results obtained in the entire temperature (10–300 K) and field (0–1.4 T) ranges on the same samples were interpreted in the light of recent developments concerning current transport in HTSC's.

In the normal state, the physics of current transport seems to be contained in the T^2 dependence of the cotangent of the Hall angle. Three models can account qualitatively for such a dependence: a bipolaron model, a BCS model with a Van Hove singularity, and RVB theory. More precise quantitative analysis of these models is required to establish which of them is correct. However, in view of recent evidence for the existence of Van Hove singularities in the electronic density of states of HTSC's, the most plausible explanation of the transport properties of HTSC's may be the BCS mechanism in the presence of a singularity near the Fermi level.

Superconducting fluctuations studies, both in the resistivity and the Hall effect, have been analyzed in connection with the Lawrence-Doniach and Fukuyama-Ebisawa-Tsuzuki models of Aslamasov-Larkin fluctuations. The strongly two-dimensional character of films of the 2:2:1:2 compound is demonstrated from both measurements. The only parameter in the model for resistivity fluctuations is the effective spacing between superconducting planes, which is found to be 8.5 Å, but this value may have been influenced by the granular character of the films.

The sign reversal of the Hall effect in the vortex state of Bi-Sr-Ca-Cu films is assigned to vortex motion. It is a common feature of all high- T_c superconductors. An explanation based on the motion of defects in two-dimensional vortex lattice bundles yields a calculated activation energy which agrees well with the measured value of 750 K. Below T_c the model yields a positive sign for the Nernst voltage (due to the motion of vortex lattice bundles) and a negative sign for the Hall voltage (due to the motion of defects in the vortex bundles).

ACKNOWLEDGMENTS

We would like to express our gratitude to Michel Lagues for the use of the facilities available in the “Laboratoire de Physique Quantique” of the ESPCI, Paris. We also acknowledge useful discussion with Charles Simon, Michel Lagues, Julien Bok, and Guy Deutscher.

- ¹T. T. M. Palstra, B. Batlogg, R. B. van Dover, L. F. Schneemeyer, and J. V. Waszczak, *Phys. Rev. B* **41**, 6621 (1990).
- ²Y. Iye, S. Nakamura, and T. Tamegai, *Physica C* **159**, 616 (1989).
- ³S. J. Hagen, C. J. Lobb, R. L. Greene, M. G. Forrester, and J. Talvacchio, *Phys. Rev. B* **42**, 6777 (1990).
- ⁴J. Luo, T. P. Orlando, and J. M. Graybeal, *Phys. Rev. Lett.* **68**, 690 (1992).
- ⁵T. R. Chien, T. W. Jing, N. P. Ong, and Z. Z. Wang, *Phys. Rev. Lett.* **66**, 3075 (1991).
- ⁶J. P. Rice, J. Giapintzakis, D. M. Ginsberg, and J. M. Mochel, *Phys. Rev. B* **44**, 10 158 (1991).
- ⁷T. R. Chien, D. A. Brawner, Z. Z. Wang, and N. P. Ong, *Phys. Rev. B* **43**, 6242 (1991).
- ⁸C. Kendziora, D. Mandrus, L. Mihaly, and L. Forro, *Phys. Rev. B* **46**, 14 297 (1992).
- ⁹M. Viret, J. F. Lawler, and J. G. Lunney, *Supercond. Sci. Technol.* **6**, 490 (1993).
- ¹⁰N. F. Mott, *Contemp. Phys.* **31**, 373 (1990).
- ¹¹N. Usui, T. Ogasawara, K. Yasukochi, and S. Tomoda, *J. Phys. Soc. Jpn.* **27**, 574 (1969).
- ¹²P. W. Anderson, *Phys. Rev. Lett.* **67**, 2092 (1991).
- ¹³K. Gofron, J. C. Campuzano, R. Liu, H. Ding, D. Koelling, A. A. Abrikosov, B. Dabrowski, and B. W. Veal (unpublished).
- ¹⁴J. Labbé and J. Bok, *Europhys. Lett.* **3**, 1225 (1987).
- ¹⁵W. E. Lawrence and S. Doniach, in *Proceedings of the 12th International Conference on Low Temperature Physics*, edited by E. Kanda (Academic Press of Japan, Tokyo, 1971).
- ¹⁶A. Chéenne, R. M. Défourneau, C. Le Fiblec, J. Perrière, A. Raboutou, P. Peyral, C. Lebeau, J. Rosenblatt, and J. P. Burin, in *Proceedings of the ICAM '91 and EMRS Spring Meeting*, edited by L. Correr (Elsevier, New York, 1991), p. 567.
- ¹⁷S. Labdi, S. Metgert, and H. Raffy, in *Proceedings of the ICAM '91 and EMRS Spring Meeting* (Ref. 16), p. 37.
- ¹⁸J. Rosenblatt, A. Raboutou, P. Peyral, and C. Lebeau, *Rev. Phys. Appl.* **25**, 73 (1990).
- ¹⁹R. K. Nkum and W. R. Datars, *Phys. Rev. B* **44**, 12 516 (1991).
- ²⁰G. Balestrino, M. Marinelli, E. Milani, L. Reggiani, R. Vaglio, and A. A. Varlamov, *Phys. Rev. B* **46**, 14 919 (1992).
- ²¹H. Fukuyama, H. Ebisawa, and T. Tsuzuki, *Prog. Theor. Phys.* **46**, 1028 (1971).
- ²²A. T. Dorsey and M. P. A. Fisher, *Phys. Rev. Lett.* **68**, 694 (1992).
- ²³S. N. Artemenko, I. G. Gorlova, and I. Yu. Pis'ma Zh. Eksp. Teor. Fiz. **49**, 352 (1989).
- ²⁴A. Freimuth, C. Hohn, and M. Galfy, *Phys. Rev. B* **44**, 10 396 (1991).
- ²⁵H. J. Jensen, P. Minnhagen, E. Sonin, and H. Weber, *Europhys. Lett.* **20**, 463 (1992).
- ²⁶S. N. Artemenko, I. G. Gorlova, and Yu. I. Latzshev, *Physica C* **193**, 47 (1992).
- ²⁷S. Martin, A. T. Fiory, R. M. Flemming, G. P. Espinosa, and A. S. Cooper, *Phys. Rev. Lett.* **62**, 677 (1989).
- ²⁸P. Nozières and W. F. Vinen, *Philos. Mag.* **14**, 667 (1966).
- ²⁹J. Bardeen and M. J. Stephen, *Phys. Rev. A* **140**, 1197 (1965).
- ³⁰M. Kosterlitz and D. J. Thouless, *J. Phys. C* **6**, 1181 (1973).
- ³¹S. J. Hagen, C. J. Lobb, R. L. Greene, M. G. Forrester, and J. Talvacchio, *Phys. Rev. B* **42**, 6777 (1990).
- ³²S. J. Hagen, C. J. Lobb, R. L. Greene, and M. Eddy, *Physica C* **185-189**, 1769 (1991).

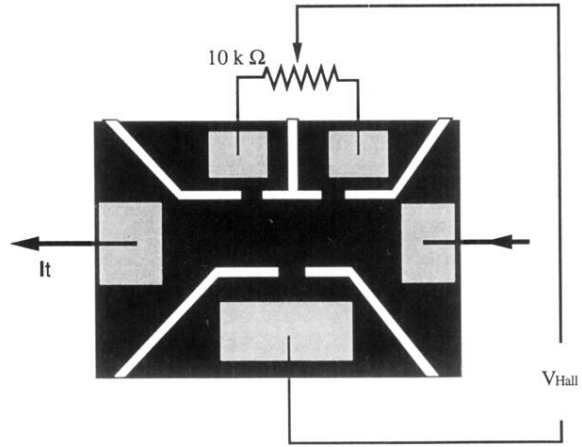


FIG. 1. Five-contact bar shape etched on the films for Hall-effect measurements.

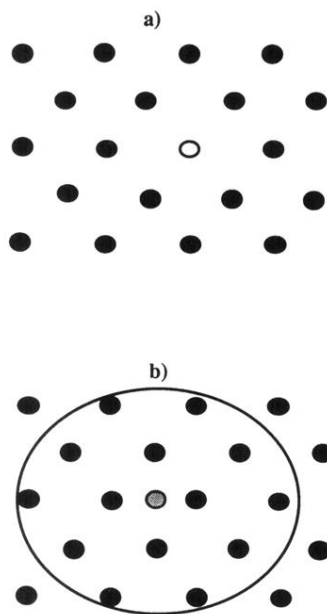


FIG. 13. Antivortex motion in a vortex lattice bundle: The energy barrier is given by the difference in energy between (b) and (a) situations. The calculation is made by considering the interaction between the antivortex and vortices contained in the ellipse of (b).